DOI: 10.1021/ma901893h

Macromolecules
ARTICLE

Understanding the Lithium Transport within a Rouse-Based Model for a PEO/LiTFSI Polymer Electrolyte

Diddo Diddens,*[,†,‡] Andreas Heuer,[†,‡] and Oleg Borodin[§]

[†]*Institut für physikalische Chemie, Westfälische Wilhelms-Universität Münster, Corrensstrasse 30, 48149 Münster, Germany,* [‡]*NRW Graduate School of Chemistry, Corrensstrasse 36, 48149 Münster, Germany, and* [§]*Department of Materials Science & Engineering, 122 South Central Campus Drive, Room 304, University of Utah, Salt Lake City, Utah 84112-0560*

Received August 26, 2009; Revised Manuscript Received December 11, 2009

ABSTRACT: MD simulations of poly(ethylene oxide) (PEO) doped with lithium-bis(trifluoromethane)sulfonimide (LiTFSI) are analyzed with respect to the cation dynamics, the PEO dynamics as well as their coupling. Different cation transport mechanisms can be identified. These observations can be interpreted in terms of a recently proposed model of cation transport in polymer electrolytes. The model was capable of reproducing the lithium mean square displacement and self-diffusion coefficient. Because of the importance of interchain ion transfers for long-range ion transport, additional focus lies on the analysis of cations coordinated by two PEO chains, which is a common motif in this system.

1. Introduction

Solid polymer electrolytes are of fundamental relevance for technological devices like batteries or fuel cells. The first studied polymer electrolytes consisted of poly(ethylene oxide) (PEO) doped with various lithium salts.[1]

For technological applications a high fraction of free ions is an important criterion, as they contribute to the net charge transport. Traditionally used lithium salts like $LiBF_4$, $LiPF_6$ or Li−triflate tend to crystallize in the electrolyte, especially at higher temperatures, whereas at lower temperatures the observed conductivity is too low for efficient technological use. Dissolving lithium salts with big anions such as lithium bis(trifluoromethane)sulfonimide (LiTFSI), the aggregation can be suppressed as the negative charge can be delocalized over the whole anion rendering ion pairs less stable.

Since the discovery of polymer electrolytes a wide variety of polymer salt systems has been studied.[2] Design of the chemical structure of the polymer host gives many possibilities to change the properties of the network such as cross-linking or the use of comb-branched polymers. Other modifications can be achieved by mixing them with other compounds, such as the addition of nanoparticles or organic solvent molecules. Immobilization of the anions by supermolecular additives can be used to raise the lithium-ion transference number, which is generally relatively low in PEO−salt systems and thus limiting their applicability.[3] Moreover, recent studies showed that also crystalline PEO−salt systems can be tuned to yield ion-conducting materials.[4] Decoupling of the ionic conductivity from the polymer mobility in semicrystalline samples has been recently discussed for PEO/$LiClO_4$,[5] while dielectric measurements[6,7] provided details on the coupling between the local polymer relaxation and the ion transport.

Various ion transport mechanisms have been discussed in the past. One important feature is the observed coupling of polymer and ion dynamics,[8] as the cations are locally bound to the polymer chains which show significant motion above their glass transition temperature. Related to the former, models such as the dynamic bond percolation (DBP) model[9] emphasize that local structural relaxation finally enables diffusive behavior of the cations. A detailed understanding of the ion transport mechanisms could thus play an important role in designing polymer electrolytes and in the predicting their macroscopic properties.

Here, molecular dynamics simulations provide a useful tool to gain basic insights in these transport mechanisms. As in experiments, PEO based electrolytes containing lithium salts have been widely studied via MD simulations,[10−13] but few simulations were able to give a more detailed picture of ion dynamics. Of course, the temperature must be high enough so that the relevant ion transport occurs during the accessible time scale of a few hundreds of nanoseconds. Furthermore, an appropriate force field is important in order to gain reliable results. Especially the incorporation of polarization promises a significant improvement in describing ion dynamics.[14−17] Basically three different cation transport mechanisms have been observed in MD simulations: Diffusion of the cation along the polymer chain, cooperative motion of the cation with the polymer chain and cationic transfer between different polymer chains.

While all of these mechanisms were observed even in early simulation studies of PEO/Li salt electrolytes,[11,18] only relatively recent work has resulted in a quantitative characterization of each contribution to the lithium diffusion andthe correlation between them.[19,20] Borodin et al.[19] have extracted the lithium diffusion coefficient along PEO chains, the rate of interchain (intersegmental) hopping, and the characteristic parameter for the lithium motion with the polymer segment on the time scale shorter than the Rouse time. The latter was described via the mean square displacement $MSD(t) = a(c,T)t^{0.6}$, where a is a function of the salt concentration and the temperature. These three components were combined in a microscopic model similar in spirit to the DBP model of Ratner.[9] This microscopic model was found to adequately reproduce the overall lithium motion extracted from MD simulations and experimentally measured lithium self-diffusion coefficients. The work of Maitra and Heuer[20] significantly improved the approach of Borodin et al.,[19]

*To whom correspondence should be addressed. E-mail: d.diddens@uni-muenster.de.

 Published on Web 01/25/2010

which required Monte Carlo simulations to solve the microscopic model of the lithium transport. On the basis of MD simulations of a PEO/$LiBF_4$ electrolyte, the lithium transport was described by an analytical Rouse-based model. The different transport mechanisms and the time scale associated with each mechanism were similar in spirit to the microscopic model of Borodin et al. and were defined in the following way: (1) Motion of the ion takes place along the polymer backbone. The time scale the ion needs to explore the total polymer chain is denoted by τ_1. (2) The ion moves cooperatively with the polymer segments. This motion can be separated into the polymer center of mass motion and the internal polymer dynamics with the characteristic time scale τ_2. (3) Transfer between two PEO molecules takes place. The average residence time of the ion is denoted by τ_3. Moreover, correlations of motion along the chain and the polymer dynamics are incorporated in this model, making it possible to estimate the dependence of the cationic diffusion coefficient on the polymer chain length N, while the model of Borodin et al. did not explicitly depend on N.

In this contribution we apply an analytical Rouse-based model to a PEO/LiTFSI polymer electrolyte model system. In the process of parametrization of the Rouse-based model we provide additional details on the lithium transport mechanism that were not present in the previous analysis,[19] especially the detailed mechanism of cationic transfer between different PEO chains.

This article is structured as follows: In section 4 the cooperative motion of the cations with the polymer chains is investigated (in particular mechanism 2 defined above). Section 5 deals with all types of cationic motion relative to the polymer chain, i.e. mechanisms 1 and 3. In section 6, the predictions of the transport model are compared with experimental data. In section 7, we conclude.

2. MD Simulation Methodology

The previous analysis of PEO/$LiBF_4$ was based on a trajectory at $T = 450$ K with a salt concentration of ether oxygen (EO): Li = 20:1. Whereas PEO/LiTFSI was simulated at various temperatures and salt concentrations, we focus on a trajectory at $T =$ 423 Kwith a salt concentration of EO:Li = 20:1 in the current analysis, as the time scale resembles that of the PEO/$LiBF_4$ electrolyte. All simulations were performed with the MD-simulation package Lucretius[21] using a quantum chemistry based many-body polarizable force field for PEO/LiTFSI.[15,16] Here we just briefly summarize the main simulation parameters, as a more detailed description is given in ref 19. The cubic simulation cell with a box length of 35−37 Å contained 10 PEO chains with $N =$ 54 monomers each and 27 LiTFSI molecules. A Nosé-Hoover thermostat was used for temperature regulation. All bonds were constrained to their equilibrium length using the SHAKE algorithm. The trajectory was about 27 ns long and was run both as NpT and NVT ensemble.

3. Structural Properties

As already discussed in ref 19, a lithium ion was typically coordinated by 4 to 5 EOs in the simulations. Comparable values for the coordination number were also found in NDIS experiments[22] of a PEO/LiTFSI electrolyte, and also the avergage length of the Li−O bond ($r_{LiO} = 1.97$ Å) is in good agreement with the experimental data ($r_{LiO} = 2.1$ Å).[22] In case of PEO/LiTFSI two kinds of coordinations were observed (Figure 1): ions that coordinated to a contiguous part of one PEO molecule and ions coordinating to two different PEO molecules or to two separate regions of one PEO molecule. In total approximately 50% of the lithium ions were complexed by a few contiguous EOs of one chain, while the other half was bound to two chains with 2−3 EOs each. Similar binding energies for both coordination

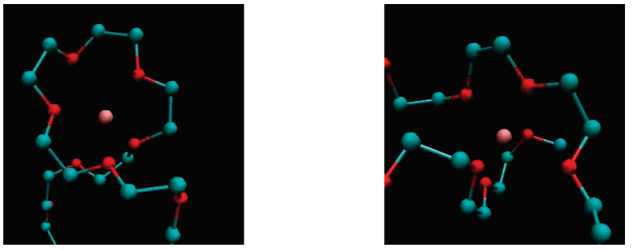

(a) (b)

Figure 1. Typical coordination environments of the lithium ions in the MD simulations: (a) lithium ion coordinated to a contiguous set of one PEO chain; (b) lithium ion coordinated to two PEO chains.

types have also been found in quantum chemistry calculations,[23] thus showing that the ratio between both coordination types in the MD simulations is reasonable. Only a small fraction (7−13%) of the lithium ions was coordinated to $TFSI^-$ anions, and those complexes only had a short lifetime, indicating the suppressed aggregation of salt in PEO/LiTFSI compared to PEO/$LiBF_4$, where about 50% of the cations were coordinated by at least one anion.

The main structural difference between the PEO/LiTFSI electrolyte and the PEO/$LiBF_4$ electrolyte from ref 20 was that the complexation of a cation by two PEO chains was much less present in PEO/$LiBF_4$, i.e., only during interchain ion transfer. This feature might originate from the fact that, in PEO/$LiBF_4$, many PEO-coordinated cations are additionally coordinated to an anion, which would make the coordination of a second PEO chain impossible, but also polarization effects could play a role.

4. Correlation of Polymer and Cation Dynamics

The local structural and dynamical properties of the PEO chains are highly affected by the proximity of ions, whereas the local structure and dynamics of regions with no ions in the proximity are basically the same as in neat PEO melts. Because of attached ions, the local polymer motion is slowed down, as the binding of several EOs to the ion reduces the number of torsional degrees of freedom of the polymer backbone, and the whole polymer-ion complex moves cooperatively. Apart from local dynamical effects, the presence of salt also accounts for changes in global polymer structure and dynamics such as a shorter end-to-end vector and a longer Rouse time. The decrease of the end-to-end vector upon adding salt to a PEO melt has also been observed in experiments.[24] The polymer dynamics itself can be separated into internal chain dynamics and center of mass motion, the latter becoming less effective in facilitating lithium transport with increasing chain length. In the following, we write for the total lithium diffusion coefficient D_{Li}

$$D_{Li} = D_M + D_{c.o.m.} \quad (1)$$

where D_M contains the lithium motion due to the three transport mechanisms as predicted by the model, whereas $D_{c.o.m.}$ contains the center of mass motion of the PEO chains, which can be determined empirically.

In order to quantify the local dynamics of the cations caused by the polymer motion, the mean square displacement (MSD) of the EOs relative to the polymer chain's center of mass was determined, on the one hand for all EOs irrespective of the possible presence of an ion, and on the other hand for EOs bound to an ion. In order to improve statistics especially at longer times where Rouse dynamics are expected to become important, we counted all events where an ion was attached to the given EO for at least 85% of the observation time. In order to evaluate the dynamical effect on the EOs by cations connected to a second PEO chain, we

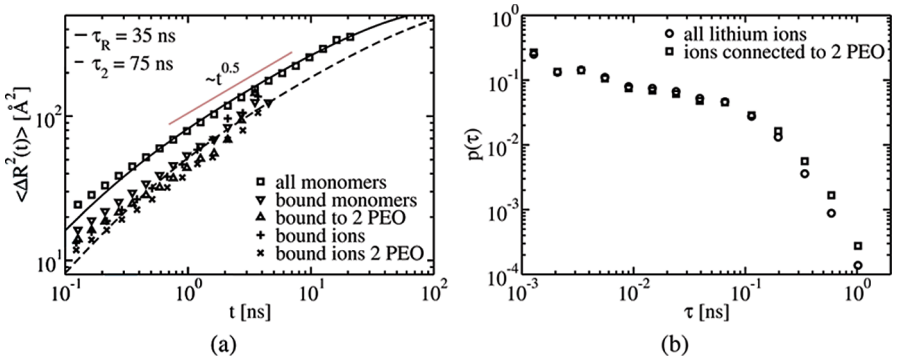

Figure 2. (a) Mean square displacement of average EOs (squares) and EOs bound to a lithium ion (triangles) relative to the polymer chain's center of mass and mean square displacement of the attached ions. (b) Distribution of Li−EO residence times τ.

determined the MSD on the one hand for all bound EOs and on the other hand only for EOs bound to an ion that is connected to two PEO chains. The MSD of the monomers relative to the polymer chain center of mass within the Rouse theory is given by

$$\langle \Delta \mathbf{R}^2(t) \rangle = \frac{2Nb^2}{\pi^2} \sum_{p=1}^{N-1} \frac{1 - \exp\left(-\frac{p^2 t}{\tau_R}\right)}{p^2} \propto \sqrt{t} \qquad (2)$$

where τ_R denotes the Rouse time and p the mode number (in total, 18 modes were used for the current system, which is approximately the number of Rouse segments we obtain with a characteristic ratio of $C_\infty = 3.4$). The proportionality holds for $\tau_R/N^2 \ll t \ll \tau_R$. The MSD for all EOs and for bound EOs as well as theoretical predictions from eq 2 (no least-squares fits) are shown in Figure 2a. In the following, the Rouse time of the average EOs will be denoted by τ_R, and the Rouse time of the bound EOs by τ_2, respectively. Additionally, the distribution of lifetimes τ, that an ion resides at a given EO, was computed and is shown in Figure 2b. This quantity again was calculated for all bound EOs and for EOs bound to an ion that is connected to two PEO chains, respectively.

We observe a Rouse-like behavior for the mean square displacement of the average EOs for longer times with a Rouse time of approximately $\tau_R = 35$ ns with a proportionality of $\langle \Delta \mathbf{R}^2(t) \rangle \propto t^{0.5}$. For short times the estimation given by the Rouse theory is lower than observed in the simulation as the real polymer has more local degrees of freedom than a simplistic bead−spring chain. For the dynamics of the bound monomers, the MSD at short time scales is also found to be above the theoretical prediction, indicating that the local PEO backbone atoms, although slowed down by attached ions, undergo conformational changes. Additionally, the cooperative rotational movement of the lithium ion together with its coordinating EOs within the picosecond regime, as discussed in ref 25, contributes to MSD at short time scales.

From about 300 ps one observes a Rouse-like behavior and thus allowing us to estimate the effective Rouse time of EOs attached to ions by eq 2, yielding a time scale of $\tau_2 = 75$ ns. That is approximately twice the time scale τ_R of the average monomers. Note that statistics becomes worse with increasing observation time t as the ions undergo movement along the chain and interchain hopping in the meantime. The MSD of EOs attached to ions that are connected to two chains lags behind the curve of the average bound EOs, but also exhibits effective Rouse dynamics.

Cations binding to two PEO chains can be regarded as cross-linkers forming a polymer network from linear PEO chains. However, it is questionable how effective these cross-links are, as the ion bound to two chains still can move along each chain separately and be detached from one chain after a certain time. The distribution of lifetimes τ that a given ion is coordinated to the same EO is shown in Figure 2b. One observes for both coordination types that most Li−EO residence times are in the picosecond regime, and that no cation is attached to a given EO for longer than a nanosecond. However, many EOs reenter the coordination shell of the cation after a short time (cf. Figure 9 in ref 19), and thus the effective cross-linking is still present. Especially for ions coordinated to the same two PEO chains during the total simulation length it is questionable if their dynamics can be captured by the analytical model from ref 20, as the contribution of the polymer dynamics will lie far below the Rouse prediction. This effect will be discussed further in section 6.

Additionally, we determined the MSD of the ions attached to the bound EOs, i.e. regarding all ions whose mean EO index (see next section) on the regarded chain changed no more than $|\Delta n| = 1$ (Figure 2a, note that for ions bound to two PEO chains the MSD was calculated in the center of mass frame of the chain with $|\Delta n| \leq 1$). At short time scales the MSDs of the ions lag behind those of the EOs, as the PEO backbone atoms have torsional degrees of freedom and the oligoether segments complexed by lithium ions undergo local rotational motion.[25] At longer times the MSDs of the ions seemingly catch up with the EO-MSDs, thus showing the combined motion of the ion with the polymer segment (note that statistics become worse with increasing observation time).

5. General Cation Dynamics relative to the Polymer Chains

In order to gain first insights into the cation dynamics relative to the polymer chain it is useful to determine the coordination environment of a given lithium ion as a function of time, as done in ref 19 (see supporting material of this paper). In the following, an EO and a cation are considered as bound if the Li − O distance is not bigger than 3 Å. Accordingly, anions and cations were regarded as bound if the Li−N($TFSI^-$) distance was not bigger than 5 Å. In total, we observe strong heterogeneities in the dynamics of the lithium ions. Some ions undergo several interchain jumps, thus traveling faster through the electrolyte, while others remain coordinated to the same PEO chain or the same two PEO chains during the whole simulation time. Cations coordinated to one chain only also briefly coordinate to anions, but no clear pattern of ion movement could be observed for these coordinations.

Additionally, cations undergo a movement along the chain by loosening from an EO on one end of their coordination sphere and forming a new bond with an EO on the other end. This mechanism is found both for ions coordinated to one PEO chain as well as for ions coordinated to two PEO chains.

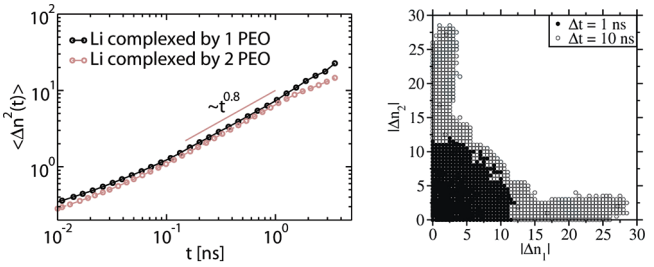

Figure 3. (a) Mean square difference of the average EO index $\langle \Delta n(t)^2 \rangle$ as a function of time. (b) Observed absolute differences of the mean EO indices $|\Delta n_1|$ and $|\Delta n_2|$.

Transport along the Chain. As mentioned above, cations can move along the PEO backbone. In principle, this type of motion can be regarded as a one-dimensional random walk along the PEO chain. In order to describe the position of the cation relative to the PEO chain, we calculate the average index n of the EOs that bind to it. The difference of the EO index Δn, after the observation time t, can be used to quantify the cationic motion relative to the polymer chain. We analyze this mechanism for ions that move along one PEO chain only and for ions that move along two PEO chains separately. For ions connected to one PEO chain, one also observes very brief coordinations of a second chain for a few picoseconds only. However, as these encounters are not expected to influence the motion along the chain significantly and in order to improve statistics, we regarded all events where the ion was bound for at least 95% of the observation time to one chain only. In case of ions connected to two chains only ions that were bound to two chains during the whole observation time t were regarded.

The average quantity $\langle \Delta n(t)^2 \rangle$ for cations that bind to one or two PEO chains is shown in Figure 3a. We observe a subdiffusive behavior for this motion from about 100 ps, i.e., $\langle \Delta n(t)^2 \rangle \propto t^{0.8}$, irrespective of the coordination of the cations by one or two PEO chains. Ions connected to two chains only lag slightly behind those coordinated to one chain, but no qualitatively different behavior could be found. Only after several nanoseconds both curves diverge seemingly, but also statistics become worse at this point. Subdiffusive behavior was also observed in our previous MD studies of PEO/$LiBF_4$, where a similar scaling was found.

To examine if the motions along each chain are correlated or independent of each other, the absolute displacements $|\Delta n_1|$ and $|\Delta n_2|$ along each chain were calculated and plotted versus each other for $\Delta t = 1$ ns and $\Delta t = 10$ ns (Figure 3b). Only ions that were connected to the same two chains during the whole observation time t were regarded.

We observe for $\Delta t = 1$ ns that some ions move basically along one PEO chain only, while others move significantly along both chains. The same behavior is observed when assuming a statistical process with uncorrelated hopping propabilities on both chains, indicating that the cation motion along each PEO chain is independent of each other at this time scale. After a longer time of $\Delta t = 10$ ns those events where the ion covers a long distance along one chain and only a short distance along the other chain become more important. This behavior might arise from structural properties, as the EOs attached to the ion will move with it cooperatively. If an ion moves a long distance along both chains, the reorganization of the polymer host will be more complicated and the dissociation of the complex will be more likely, giving rise to complexes where the ion only moves significantly along one chain.

The time scale, τ_1, an ion needs to travel from one end of the PEO chain to the other can be estimated by assuming a one-dimensional random walk motion of the ion on the polymer chain. We obtain (for the motivation of the factor π^2 see ref 20)

$$\tau_1 = \frac{(N-1)^2}{\pi^2 D_1} \tag{3}$$

where the effective diffusion coefficient D_1 for this movement can be calculated out of Figure 3a by using

$$D_1 = \frac{\langle \Delta n^2(t) \rangle}{2t} \tag{4}$$

In the following, we ignore the slight deviations from diffusive behavior in Figure 3a, as the motion will cross over to the diffusive regime after a sufficiently long time (note that even for the longest observation time in Figure 3a the displacement is on average 4−5 monomers, so that it is likely that its dynamics is still correlated to its past due to local structural effects, which will be of no importance when going to larger displacements).

In order to make the error caused by the subdiffusivity in D_1 s small as possible, we estimated D_1 at $t \approx 1.2$ ns, using a time scale that is as long as possible and still has sufficiently good statistics. Extracting D_1 from the distribution function of Δn, $p(\Delta n)$, that was found to be Gaussian to a good approximation, gives similar values for D_1, thus additionally validating our description of this type of motion. Note that the diffusion coefficient for the motion along the chain in ref 19 is approximately 2−3 times as high as in the present analysis (cf. Table 2 in ref 19). This discrepancy originates from the different method of determination of the diffusion coefficient D_1 as well as the different dependence of the slightly different model from ref 19 on D_1. The estimated values for τ_1 were $\tau_1 = 79$ ns for ions connected to one PEO chain only and $\tau_1 = 89$ ns for ions connected to two PEO chains, respectively. Ions connected to one chain only move about 10−20% faster than those connected to two chains.

Intermolecular Ion Transfer. According to the dynamic bond percolation (DBP) model, the relaxation of the polymer surroundings play a major role in the long-range ion transport. Within this model these relaxation processes serve as renewal processes, i.e., ionic pathways blocked before become accessible and vice versa. Ion dynamics are uncorrelated to past events after such a process takes place. Our previous work on PEO/$LiBF_4$ showed that the ionic transfer between two PEO chains rather than relaxation of the polymer surroundings reflects the renewal process and thus contrasts common DBP approaches. The next point of our analysis is therefore the determination of the residence time τ_3 of an ion on a given PEO chain. For PEO/$LiBF_4$, a renewal time of $\tau_3 = 110$ ns was found. Because our trajectory is relatively short compared to the expected value for τ_3, we determined the jump frequency in our simulations to give an estimate for the average residence time, though with a large uncertainty. Only real renewal events where the ion was totally transferred to another PEO chain permanently and thus became independent of its past were counted, leaving out events where the ion jumped back to the first chain immediately.

The average residence time for PEO/LiTFSI calculated from the jump rates was $\tau_3 = 49$ ns, which is even shorter than the time scales associated with intramolecular in transport ($\tau_3/\tau_2 = 0.65$, deviations from $\tau_3 = 47$ ns in ref. 19 arise

Table 1. Estimated Values for τ_1, τ_2, and τ_3 for Both Coordination Types as Well as the Values for PEO/$LiBF_4$ Taken from Ref 20

coordination	τ_1 [ns]	τ_2 [ns]	τ_1/τ_2	τ_3 [ns]	τ_3/τ_2
1 PEO	79	75	1.05	49	0.65
2 PEO	89	75	1.19		
PEO/$LiBF_4$ (N = 48)	150	42	3.57	110	2.62

from the uncertainties of the determined jump rates). Compared to PEO/$LiBF_4$, where $\tau_3/\tau_2 = 2.62$ was found, the transfer rate is significantly higher for PEO/LiTFSI. A higher rate of interchain transfer due to polarization effects has also been observed[14] by directly comparing simulations of an PEO/$LiBF_4$ electrolyte with and without polarization effects, thus highlighting the general feature that incorporating polarization yields faster ion dynamics. Moreover, in simulations incorporating polarization, lithium ions are on average coordinated to fewer EOs (4−5 for PEO/LiTFSI) than lithium ions in nonpolarizable simulations (6−7), thus making it easier to separate a cation from a given chain. Apart from polarization effects, the reason for this behavior can also be found in the structural differences between the electrolytes. In PEO/$LiBF_4$ the cations were coordinated mostly by one PEO chain only, except during a brief period when the ion was transferred to another chain, while in PEO/LiTFSI approximately 50% of the lithium ions were coordinated by two PEO chains. Thus, the coordination structure that is vital for the ion transfer is more likely formed in PEO/LiTFSI, resulting in a shorter τ_3.

Table 1 gives an overview of all three characteristic time scales. According to the model from ref 20 the contribution D_M of the three transport mechanisms to the cation diffusion coefficient defined in eq 1 in the limit of long chains can is given by (calculational details below)

$$D_M = \frac{\langle \mathbf{R}_e^2 \rangle}{6\pi}\sqrt{\frac{1}{\tau_3 \tau_{12}}} \tag{5}$$

where τ_{12} is given by the inverse of the time scale for the motion along the chain τ_1 and of the effective Rouse time τ_2 of the bound EOs

$$\frac{1}{\tau_{12}} = \frac{1}{\tau_1} + \frac{1}{\tau_2} \tag{6}$$

The ratio τ_1/τ_2 measures the relative importance of motion along the chain and of motion due to polymer dynamics to the total intramolecular cation dynamics. This measure motivates the factor π^2 in the definition of τ_1 in eq 3, as both time scales τ_1 and τ_2 become directly comparable. We observe $\tau_1 \approx \tau_2$ for both coordination types, indicating that both polymer relaxation and motion along the chain contribute significantly to intramolecular ion motion. Contrary to this, a significantly different ratio of $\tau_1/\tau_2 = 3.57$ for PEO/$LiBF_4$ shows that motion along the chain is much more important in PEO/LiTFSI. The reason for this difference may also lie in the usage of a polarizable force field and thus faster ion dynamics for PEO/LiTFSI, but it could also be a general feature of the PEO/LiTFSI system since no simulation data of PEO/$LiBF_4$ with a polarizable force field was available for comparison. The major importance of transport along the chain for PEO/LiTFSI is also underlined by the fact that no cation resides at a given EO longer than a nanosecond (Figure 2b). The importance of intramolecular ion transport relative to the renewal processes is measured by the ratio τ_3/τ_2. In the limit of short chains (but not too short chains, i.e., approximately $10 < N < 80$, see section 6) and thus short τ_1 and τ_2 values the cation diffusion coefficient relative to the chain's center of mass is only dependent on the renewal time,[20] i.e., $D_M \propto 1/\tau_3$, in contrast to the original DBP model that predicts this proportionality for all N.[9] Although the renewal time τ_3 for PEO/LiTFSI is much smaller than for PEO/$LiBF_4$, the ratio of $\tau_3/\tau_2 = 0.65$ shows that it is still sufficiently large for a significant contribution of both intramolecular transport mechanisms. The ratio τ_3/τ_1, which also could be used to measure the importance of intramolecular transport relative to the renewal processes, is nearly identical to the ratio τ_3/τ_2 for PEO/LiTFSI. This again shows that although about 50% of the ions are coordinated by two different PEO chains, they still diffuse along each chain significantly and thus travel a certain distance before a renewal event takes place.

Having determined all three time scales, we are now able to reproduce the lithium MSD determined from the MD simulation. The MSD in the center of mass frame of the polymer chain $g_{Li}^{M12}(t)$ due to both intramolecular mechanisms (i.e., motion along the polymer chain and polymer dynamics) is given by a summation over the Rouse modes p of the polymer chain (see ref 20 for calculational details)

$$g_{Li}^{M12}(t) = \frac{2\langle \mathbf{R}_e^2 \rangle}{\pi^2} \sum_{p=1}^{N-1} \frac{1 - \exp\left(\frac{-p^2 t}{\tau_{12}}\right)}{p^2} \tag{7}$$

We modeled the lithium motion after a renewal process by a random change in direction, the distance traveled between two renewal processes was calculated by eq 7, where the times between two renewal processes were randomly sampled from a exponential distribution. In this way a numerical result for the average traveled distance after n renewal processes was obtained. The total lithium MSD in a given time t was calculated by averaging the MSDs after n renewal processes during t weighted by the Poissonian probability (with mean t/τ_3) that n renewal processes have occurred.

The values for τ_1 and τ_2 are taken from Table 1, where for τ_1 the average value for ions coordinated to one PEO chain and for ions that were coordinated by two chains was used. We observe that the curve of the model for $\tau_1 = 84$ ns and $\tau_2 = 75$ ns overestimates the MSD in the MD simulations, which is expected to be caused by cations that are coordinated to the same two PEO chains during t and thus immobilized. A separate analysis of the lithium MSDs in dependence of the coordination environment (shown in Figure 4a) shows that the diffusion along the chain for cations coordinated to the same two PEO chains during the observation time t does not effectively contribute to the lithium movement relative to the polymer chains center of mass. The MSD for cations coordinated to two PEO chains that do not move along the chain ($|\Delta n| \leq 1$, crosses in Figure 4a) as well as the MSD for ions undergoing both intramolecular transport mechanisms (triangles in Figure 4a) are nearly identical, though the displacement in terms of traveled monomer units of the latter is comparable to that of ions bound to one PEO only. In this picture the cation is held back by the second polymer chain, while the chain passes reptation-like along the ion, so that the absolute displacement of the ion is small. This is also consistent with the observation in Figure 3b where the absolute monomer index $|\Delta n|$ basically changes on one chain only. Contrarily, the MSD for lithium ions coordinating to one individual PEO chain only during t (temporary coordinations of other chains were allowed) is in good agreement with the model prediction. The overall intramolecular lithium motion is thus a superposition of two different transport types. Both contributions

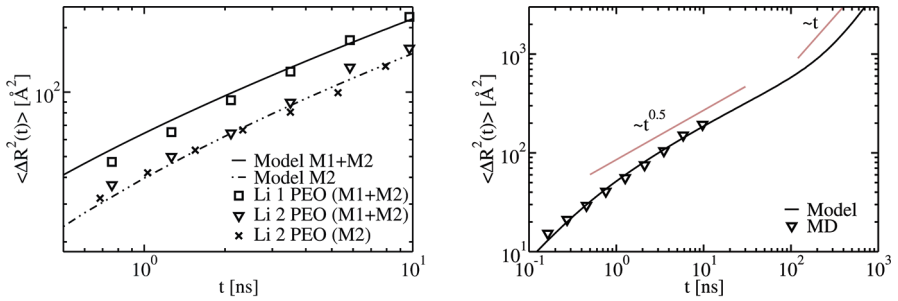

Figure 4. Mean square displacements of the lithium ions relative to the polymer chain's center of mass from the MD simulation (symbols) and the transport model (solid line) for different coordination environments and the two different transport mechanisms M1, M2 (M1, diffusion of the cation along the PEO chain; M2, polymer dynamics of bound EOs that facilitates the coordinated cations). The dash-dotted line corresponds to the model curve regarding polymer dynamics (M2) only with $\tau_2 = 95$ ns.

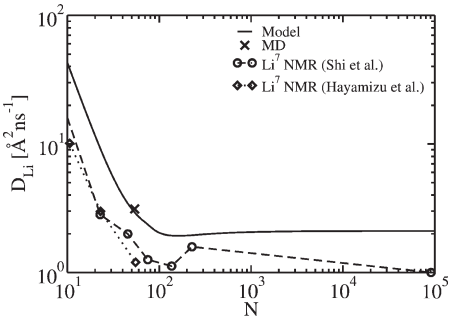

Figure 5. Lithium diffusion coefficient D_{Li} in dependence of the polymer chain length N predicted by the transport model and experimental PFG-NMR measurements of a PEO/LiTFSI system (EO: Li = 20: 1) at $T = 363$ K from Shi et al.[26] (circles) and Hayamizu et al.[27] (diamonds).

can be expressed by eq 7 with $\tau_1 \rightarrow \infty$ for ions coordinated to the same two chains and $\tau_1 = 79$ ns for the other ions weighted by their ratio. As ions coordinated to two chains will be detached from one chain after a certain time, the ratio changes during the observation time. Thus, additional information is required to formulate an analytical expression for the total lithium MSD. However, for practical purposes, the MSD can be reproduced by an effective value of $\tau_{12} = 64$ ns (Figure 4b) that captures this effect. The lithium motion on a time scale shorter than ~100 ps is expected to be dominated by the detailed local chemical structure and is thus not incorporated in the Rouse-like transport model.

At longer times (i.e., $t \approx 2\tau_3$), the model correctly predicts the expected crossover from subdiffusive to linear diffusive behavior (Figure 4b). Unfortunately, a crossover from subdiffusive lithium motion to diffusive lithium motion cannot be observed in the MD simulations as more than of a factor ten longer simulations would be needed. Because of the incorporation of polarization, longer simulation runs for the investigation of this crossover would be computationally too expensive.

Figure 5 shows the lithium self-diffusion coefficient $D_{Li} = D_M + D_{c.o.m.}$ in dependence of the polymer chain length N predicted by the transport model as well as determined experimentally by means of PFG-NMR of a PEO/LiTFSI system with a salt concentration of EO:Li = 20:1 at $T = 363$ K by Shi et al.[26] and Hayamizu et al.,[27] respectively. For the transport model, the contribution $D_{c.o.m.}$ of the polymer's center of mass was estimated by using three different scaling regimes as done in ref 20. For the Rouse regime ($N < 75$)[26] one expects $D_{c.o.m.} \propto N^{-1}$, however, deviations from the Rouse prediction up to $D_{c.o.m.} \propto N^{-2}$ have been reported[27−29] While in ref 20 a proportionality of $D_{c.o.m.} \propto N^{-1.7}$ was used for the calculation of D_{Li}, we use the N-scaling $D_{c.o.m.} \propto N^{-1.95}$ from ref 27 as we will compare the model predictions with experimental data from this reference in the next section. For the crossover regime ($75 \leq N < 225$) and for the entanglement regime ($N \geq 225$) we used the scalings $D_{c.o.m.} \propto N^{-3}$ and $D_{c.o.m.} \propto N^{-2}$, respectively.[30] The prefactor of the N-scaling was chosen such that $D_{c.o.m.}$ ($N = 54$) matches the value extracted from the MD simulation. The contribution D_M of the three transport mechanisms to the overall lithium diffusion coefficient was determined numerically by making use of the renewal property

$$D_M = \frac{\langle g_{Li}^{M12}(\tau)\rangle_{M3}}{6\tau_3} \tag{8}$$

where $\langle ... \rangle_{M3}$ denotes the average of eq 7 over all possible τ_3, which were assumed to be exponentially distributed (i.e., $\exp(-t/\tau_3)/\tau_3$). For the three time scales, the following N-scalings were used: $\tau_1 \propto N^2$, $\tau_2 \propto N^2$ and $\tau_3 \propto N^0$. The average $\langle g_{LI}^{M12}(\tau)\rangle_{M3}$ in eq 8 was calculated by integrating eq 7 weighted by the exponential propability distribution

$$\langle g_{Li}^{M12}(\tau)\rangle M3 = \int_0^\infty dt \frac{\exp(-t/\tau_3)}{\tau_3} g_{Li}^{M12}(t)$$

$$= \frac{2\langle \mathbf{R}_e^2\rangle}{\pi^2} \sum_{p=1}^{N-1} \frac{1}{p^2}\left[1 - \frac{1}{p^2\frac{\tau_3}{\tau_{12}} + 1}\right] \tag{9}$$

and inserting the result into eq 8 (note that in contrast to this, for derivation of the relationship in eq 5 the sum in eq 7 was approximated by an integral from 0 to ∞ with $\tau_{12} \gg \tau_3$ and the result was inserted in eq 8). We observe, similar as in ref 20, a minimum for the overall diffusion coefficient with a transition to a N-independent regime in the crossover region from the polymer center of mass-dominated diffusion to percolation-dominated diffusion ($N \approx 100$) for both curves, thus again validating the transport model. The experimental data sets are in qualitative agreement with the model prediction, however, quantitative differences can easily be explained by the different temperature in the experiments.

However, one might expect that in the limit of large N the only important parameter is τ_3, as $\tau_{12} \propto N^2$ will become infinitely large. Additionally, the polymer motion will cross over to reptation dynamics after exceeding a certain chain length N_e, which will also slow down contribution of the PEO dynamics. However, τ_{12} contributes significantly to D_M in the large-N limit on a local scale, as mean square displacement

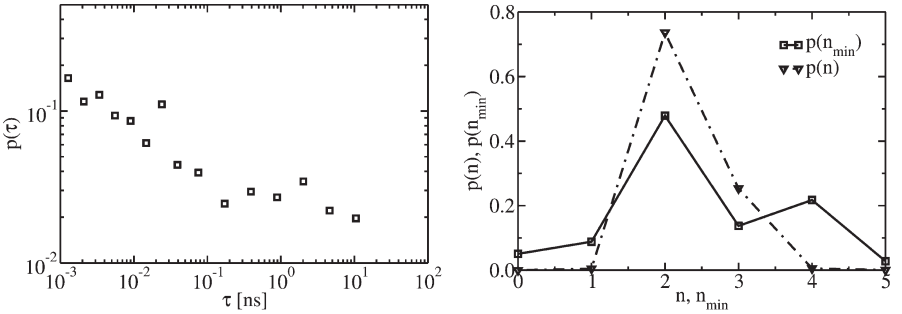

Figure 6. (a) Distribution of lifetimes of complexes where one lithium ion is coordinated by two PEO chains. (b) Distribution of coordination numbers n in these complexes (dash-dotted line) and of the minimum coordination number n_{min} that is reached during the lifetime of a complex (solid line).

of the ion between two successive renewal events is given by the intramolecular contributions (see also eq 8). Despite the fact that the polymer dynamics will experience an additional slow down in the reptation regime, the contribution of the ionic motion along the chain will remain unchanged in this case, as this motion is directed along the curvilinear path of the chain and thus is not affected by the tube constrains within the reptation picture. Thus, the contribution of the intramolecular cation transport is important especially in the limit of large N.

Although our model does not incorporate reptation dynamics, it can still be applied in the reptation case under some conditions. If the renewal time τ_3 is shorter than τ_e, which is the time scale after which the chain experiences additional constraints due to the tube imposed by the surrounding chains,[31,32] the cation dynamics is not affected by entanglement effects, as the ions are transferred to another chain before the onset of the entanglement regime. The onset time for the entanglement time τ_e can be estimated by the Rouse time of a chain of length N_e. For PEO one finds with $N_e \approx 100$ and the scaling of the Rouse time $\tau_e \approx 300$ ns, which is much larger than τ_3, so that the segmental dynamics in this case are correctly reproduced by the transport model even for large N. In cases where $\tau_3 > \tau_e$, the contribution of τ_2 becomes less important with large N, but the contribution of τ_1 remains important despite entanglement effects, as discussed above.

Because of the relevance of complexes consisting of a cation and two PEO chains for the renewal processes we analyzed them in more detail. First, we determined the distribution of their lifetimes (Figure 6(a)). As can be seen, the lifetimes of most complexes are in the picosecond regime. Only a few complexes exist for several nanoseconds. Note that some of these complexes even existed during the total simulation length (though not counted in Figure 6(a)). In the picosecond regime, the distribution of lifetimes exhibits a scaling of approximately $p(\tau) \propto \tau^{-0.4}$ whereas the complexes in the nanosecond regime are too few to make clear predictions. The observation that most complexes are short-lived gives rise to the question how an ion transfer can be established by these complexes, as the transfer process requires a certain time where the ion loosens from the first PEO chain and a stable coordination environment has to be formed by the new PEO chain.

Therefore, we investigate the process of formation and decay of these complexes in the following way. When a second PEO chain enters the coordination sphere of a cation bound to 4−5 EOs, this coordination number n becomes smaller. The minimum coordination number n_{min} of the first PEO chain that is reached within the total lifetime can thus be used to monitor the progress of the ion transfer to the second PEO chain. Furthermore, this quantity shows which fraction of all formed complexes results in a transfer of the ion, corresponding to $n_{min} = 0$. Figure 6(b) shows the probability, that a certain minimum EO coordination number n_{min} of the first PEO chain is realized during the lifetime of the complex, as well as the probability that the ion is bound to n EOs of the first PEO chain at any time during the lifetime of the complex.

The distribution $p(n)$ (Figure 6b, dash-dotted line) shows that the cations are most probably (about 54%) coordinated to $n = 2$ EOs on each chain, indicating that a symmetric coordination on both PEO chains is most stable. Other stable coordination numbers are $n = 2$ EOs of one chain and $n = 3$ EOs of the other chain (∼18%) as well as 3 EOs from each chain (∼7%), though the repulsion between the EOs makes these coordination numbers less favorable. Averaged over all lifetimes, a pair of coordination numbers of $n = 1$on one chain and $n = 4$ on the other chain is extremely unlikely and only observed in the first picoseconds a complex forms or decays.

The distribution of $p(n_{min})$ (solid line in Figure 6b) shows two maxima at $n_{min} = 4$ and $n_{min} = 2$. The maximum at $n_{min} = 4$ corresponds to unstable complexes where the second PEO chain coordinates only a few picoseconds to the cation before it detaches again, as coordination numbers of $n = 4$ (or $n = 1$ on the other chain) are very unlikely realized (dash-dotted line in Figure 6b). The other maximum for $p(n_{min})$ at $n_{min} = 2$ arises from stable complexes, as a coordination number of $n = 2$ is the most probable. Only about 5% of all complexes result in a complete ion transfer with $n_{min} = 0$. Relative to the percentage of symmetric complexes where the first chain is already relatively far detached ($n_{min} = 2$), still only ∼10% lead to an ion transfer. Additionally, we also observe even for events with $n_{min} = 0$ that the ion jumped back to the old chain after a few picoseconds, showing that not all events with $n_{min} = 0$ are renewal processes. Only about 50% of all events with $n_{min} = 0$ counted in Figure 6b were real renewal events as discussed in the previous section, reducing the amount of complexes that provide a successful renewal event to 2−3%. We can summarize, that unless the ion has not moved away from the first chain for a longer period, the ion motion is still strongly correlated to its past, as it jumps more likely back to the old chain. This emphasizes that in addition to simple ion transfer the surrounding polymer structure has to reorganize in order to prevent jumping back. This assumption would bridge the gap between the traditional DBP theory, where polymer relaxation makes up the renewal process, and the transport model from ref 20 where ionic hops were interpreted as a renewal event. A renewal mechanism combining ion transfers with subsequent polymer relaxation is implied instead.

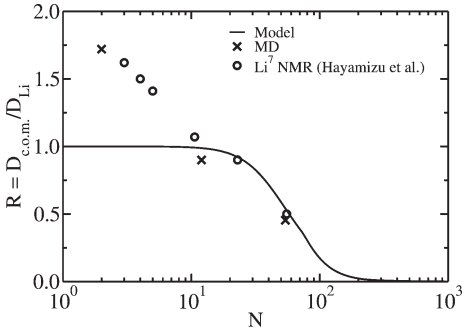

Figure 7. Relative importance R_{Li} of the PEO diffusion to the lithium diffusion in dependence of N calculated from the model (solid line) as well as experimental values from ref 27 and from MD simulations (crosses) of the current system (N = 54), PEO/LiTFSI[17] (N = 12) and DME/LiTFSI[33] (N = 2, the latter both with EO:Li = 20:1).

6. Comparison of Lithium and Polymer Dynamics

Apart from the brief validation of our transport model by comparing the N-dependence of the overall lithium diffusion coefficient extracted from both experiments and theory, we wish to analyze the capability of our model in more detail. In the following, we will compare the predictions of our model to the experimental results taken from ref 27 as well as MD simulations from this work and refs 17 and 33. In particular, we focus on the two contributions to the overall lithium diffusion coefficient, i.e., the collective diffusion of the lithium ion and the PEO chain's center of mass and the diffusion of lithium ion due to the three transport mechanisms. In order to determine their relative importance, we define the following ratio

$$R_{Li} = \frac{D_{c.o.m.}}{D_{Li}} \tag{10}$$

as done in ref 27. Figure 7 compares the values for R_{Li} calculated by the transport model (i.e., $D_{c.o.m.}/(D_{c.o.m.}+D_M)$) with the experimental values taken from ref 27. Note that, in contrast to the analysis above, $D_{c.o.m.}$ was calculated using the scaling $D_{c.o.m.} \propto N^{-1.95}$ as found in ref 27. In contrast to the absolute diffusion lithium coefficients discussed above, the authors of ref 27 found that the values of R_{Li} are nearly temperature-independent and are thus ideal for the comparison of experiment and simulation independent of temperature. Moreover, as the measurements in ref 27 were also carried out for very small N, the quantity R_{Li} can be used to test the range of applicability of our transport model, as it was developed for polymeric solvents, while for ethylene oxide oligomers a different cation transport mechanism is expected. In fact, the first three experimental values, i.e. N = 3, N = 4, and N = 5, are significantly larger than one and thus strongly differ from the model prediction, while the experimental value for N = 10.6 is in quite good agreement and the values for N = 22.9 and N = 55.3 are in very good agreement with the model prediction. Figure 7 also shows MD simulation data for N = 2,[33] N = 12,[17] and the current system (N = 54), which are also in quite good agreement with the experimental data points. When N becomes smaller than the EO: Li ratio, a certain fraction of the solvent molecules is not coordinated to a cation and thus diffuses faster, leading to $D_{c.o.m.} > D_{Li}$, as it is generally observed for organic solvents[34] as well as water,[35] and thus a R_{Li} value larger than one. The crossover length when the R_{Li} values become larger than one can be estimated for sufficiently high concentrations by $N \approx$ EO:Li. Within this regime the cooperative movement of lithium and oligoether is the dominant transport mechanism.[33] In contrast to electrolytes composed of ethylene carbonate and LiTFSI, the solvent exchange in the coordination sphere of the cations does not significantly contribute to the lithium transport for short oligoethers[33] (for N = 12 it was observed that 90% of the total lithium diffusion was due to the cooperative motion with the solvent). Thus, when using the diffusion coefficient of the complexed solvent molecules only for $D_{c.o.m.}$, we would obtain an agreement with the model curve even for smallest N.

For small solvent molecules, R_{Li} can also be interpreted within the Stokes−Einstein equation as relative ratio of the Stokes radius of the solute (i.e., the lithium ion and its surrounding coordination sphere) and the solvent molecules themselves.[27,34] By neglecting the van der Waals radius of the rather small lithium ion, the values for R_{Li} can be taken as a measure for the average number of solvent molecules within the coordination sphere of the cation, where a value of R_{Li} = 2 would mean that the lithium ion diffuses on average with two solvent molecules.[27,34] While this explanation works well for small solvent molecules,[34] it breaks down for polymeric solvents, as the cations also undergo interchain transfer processes and thus move faster, an effect not captured in the analysis of ref 27. Generally speaking, in refs 27 and 34 all transport properties of the solvent and the cations are explained by structural properties of the ion coordination environment only, while in our model the cation transport is explained by the dynamical quantities τ_1, τ_2, and τ_3 of the system, and thus, the general mechanism is independent of the detailed coordination structure. For the long time scale probed by PFG-NMR experiments, the interchain transfers are the most important contribution to D_M, irrespective of the specfic value of τ_3 which in turn is also only indirectly related to the cation coordination structure. The values $R_{Li} < 1$, meaning that the cations diffuse faster than the solvent, are hard to interpret without considering the intermolecular transfer processes. We thus emphasize that for polymeric solvents the R_{Li} values should rather be explained by the cationic transfers than by the local coordination structure. However, ion pairing might also play a role, as the degree of dissociation is only about 50% for N = 4.[27] Consistently with the simulation, the degree of dissociation increases with the chain length, where at N = 55:3 the salt is nearly totally dissolved. From the present analysis of the R_{Li} values we can state that our model can be applied in the regime where most of the solvent molecules coordinate one or more cations (i.e., from $N \approx$ EO:Li). Additionally, our model gives an explanation for the plateau value of D_{Li} for large N.

7. Conclusions

Our analysis suggests that the cation transport model developed in ref 20 for PEO/$LiBF_4$ can also be applied to the PEO/LiTFSI electrolyte despite structural differences. It could be shown that the coordination of a lithium ion by two PEO chains still allows diffusion (in terms of monomer units) of the ion along each chain independent of each other. The diffusion constants D_1 for ion transport along the chain showed only slight differences for both coordination environments. However, the displacement of a cation relative to the polymer chain in absolute space is more drastically affected by the coordination environment, as the contribution of the diffusion along the polymer chain to the real-space ion displacement is approximately zero for cations coordinated to two PEO chains, which we suppose is due to the second chain that holds the ion at a fixed position. In contrast to this, the contribution of intrachain diffusion to the lithium motion for ions coordinating to one individual chain only is adequately reproduced by the transport model. The total lithium MSD can be reproduced by a higher, effective relaxation time. The relaxation of the polymer segments showed a Rouse-like behavior both for average EOs and for bound EOs, yielding a relaxation time for bound EOs that approximately doubles compared to the Rouse time.

Cations coordinating to two PEO chains have a cross-linking effect on the polymer surroundings, affecting the polymer dynamics. However, as these cross-links are destroyed after a certain time, this effect only slightly raises the effective Rouse time τ_2 for these EOs. As in the previous analysis of the PEO/$LiBF_4$ electrolyte,[20] the N-scaling of the lithium self-diffusion coefficient predicted by the transport model and measured by PFG-NMR experiments were in good agreement. Differences in the absolute values of the lithium self-diffusion coefficient can be explained by the higher temperature in the MD simulations. Moreover, the temperature-independent R_{Li} values from theory and experiment were in very good agreement for $N \geq 10$, whereas for smaller N a different cation transport mechanism holds.

The ion transfer rate or renewal rate was much higher for the PEO/LiTFSI electrolyte, which we suppose is due to the large amount of cations complexing with two PEO chains, necessarily formed as intermediates for interchain cation transfer. Additional analysis has shown that only a small fraction of these complexes provide a renewal event in which the ion was permanently transferred and thus able to travel long distances. In most complexes, the ion jumped back to the old chain, even if it was coordinated with equal coordination numbers by both chains, indicating that the polymer host also has to reorganize in order to provide successful ion transfer. This mechanism would combine the renewal picture of polymer relaxation processes in the DBP model with the picture of ionic transfer events in the previously formulated cationic transport model.

Acknowledgment. A.H. and D.D. would like to thank the Sonderforschungsbereich 458 and the NRW Graduate School of Chemistry for financial support as well as A. Maitra for helpful correspondence. Financial support to the University of Utah was provided by the U.S. Department of Energy under contract DE-AC02-05CH11231 on PO No. 6838611.

Supporting Information Available: Various plots of the EO index vs t. This material is available free of charge via the Internet at http://pubs.acs.org.

References and Notes

(1) Bruce, P. G.; Vincent, C. A. *J. Chem. Soc. Faraday Trans.* **1993**, *89*, 3187–3203.
(2) Gray, F. M. *Solid Polymer Electrolytes*; Wiley-VCH: New York, 1991.
(3) Blazejczyk, A.; Wieczorek, W.; Kovarsky, R.; Golodnitsky, D.; Peled, E.; Scanlon, L. G.; Appetecchi, G. B.; Scrosati, B. *J. Electrochem. Soc.* **2004**, *151*, A1762–A1766.
(4) Staunton, E.; Andreev, Y. G.; Bruce, P. G. *Faraday Discuss.* **2006**, *134*, 143–156.
(5) Fullerton-Shirey, S. K.; Maranas, J. K. *Macromolecules* **2009**, *42*, 2142–2156.
(6) Fragiadakis, D.; Dou, S.; Colby, R. H.; Runt, J. *Macromolecules* **2008**, *41*, 5723–5728.
(7) Fragiadakis, D.; Dou, S.; Colby, R. H.; Runt, J. *J. Chem. Phys.* **2009**, *130*, 064907.
(8) Ratner, M. A.; Johansson, P.; Shriver, D. F. *MRS Bull.* **2000**, *25*, 31.
(9) Nitzan, A.; Ratner, M. A. *J. Phys. Chem.* **1994**, *98*, 1765–1775.
(10) Müller-Plathe, F. *Acta Polym.* **1994**, *45*, 259–293.
(11) Müller-Plathe, F.; van Gusteren, W. F. *J. Chem. Phys.* **1995**, *103*, 4745–4756.
(12) Neyertz, S.; Brown, D. *J. Chem. Phys.* **1996**, *104*, 3797–3809.
(13) Siqueira, L. J. A.; Ribeiro, M. C. C. *J. Chem. Phys.* **2005**, *122*, 194911.
(14) Borodin, O.; Smith, G. D.; Douglas, R. *J. Chem. Phys. B* **2003**, *107*, 6824–6837.
(15) Borodin, O.; Smith, G. D. *J. Chem. Phys. B* **2006**, *110*, 6279–6292.
(16) Borodin, O.; Smith, G. D. *J. Chem. Phys. B* **2006**, *110*, 6293–6299.
(17) Borodin, O.; Smith, G. D.; Geiculescu, O.; Creager, S. E.; Hallac, B.; DesMarteau, D. *J.Phys. Chem. B* **2006**, *110*, 24266–24274.
(18) Borodin, O.; Smith, G. D. *Macromolecules* **2000**, *33*, 2273–2283.
(19) Borodin, O.; Smith, G. D. *Macromolecules* **2006**, *39*, 1620–1629.
(20) Maitra, A.; Heuer, A. *Phys. Rev. Lett.* **2007**, *98*, 227802.
(21) Smith, G. D.; Ayyagari, C.; Bedrov, D.; Borodin, O. *Lucretius-V.8.0*, 2004, lucretius.mse.utah.edu.
(22) Mao, G.; Saboungi, M.-L.; Price, D. L.; Armand, M. B.; Howells, W. S. *Phys. Rev. Lett.* **2000**, *84*, 5536–5539.
(23) Baboul, A. G.; Redfern, P. C.; Sutjianto, A.; Curtiss, L. A. *J. Am. Chem. Soc.* **1999**, *121*, 7220–7227.
(24) Annis, B. K.; Kim, M.-H.; Wignall, G. D.; Borodin, O.; Smith, G. D. *Macromolecules* **2000**, *33*, 7544–7548.
(25) Duan, Y.; Halley, J. W.; Curtiss, L.; Redfern, P. *J. Chem. Phys.* **2005**, *122*, 054702.
(26) Shi, J.; Vincent, C. A. *Solid State Ionics* **1993**, *60*, 11–17.
(27) Hayamizu, K.; Akiba, E.; Bando, T.; Aihara, Y. *J. Chem. Phys.* **2002**, *117*, 5929–5939.
(28) von Meerwall, E.; Beckman, S.; Jang, J.; Mattice, W. L. *J. Chem. Phys.* **1998**, *108*, 4299–4304.
(29) Paul, W.; Smith, G. D. *Rep. Prog. Phys.* **2004**, *67*, 1117–1258.
(30) Appel, M.; Fleischer, G. *Macromolecules* **1993**, *26*, 5520–5525.
(31) de Gennes, P. G. *Scaling Concepts in Polymer Physics*; Cornell University Press: Ithaca, NY, 1979.
(32) Doi, M.; Edwards, S. F. *The Theory of Polymer Dynamics*; Oxford Science Publications: Oxford, U.K., 2003.
(33) Borodin, O.; Smith, G. D. *J. Solution Chem.* **2007**, *36*, 803–813.
(34) Hayamizu, K.; Aihara, Y.; Arai, S.; Martinez, C. G. *J. Phys. Chem. B* **1999**, *103*, 519–524.
(35) Spangenberg, D.; Hermansson, K. *J. Chem. Phys.* **2004**, *120*, 4829–4843.